Simulating the Interplay of Particle Conservation and Long-Range Coherence

Emanuele G. Dalla Torre[1,2] and Matthew J. Reagor[3,2]
[1]*Department of Physics and Center for Quantum Entanglement Science and Technology, Bar-Ilan University, 52900 Ramat Gan, Israel*
[2]*Superconducting Quantum Materials and Systems Center (SQMS), Fermi National Accelerator Laboratory, Batavia, Illinois 60510, USA*
[3]*Rigetti Computing, 775 Heinz Avenue, Berkeley, California 94710, USA*

(Received 23 June 2022; revised 13 December 2022; accepted 4 January 2023; published 10 February 2023)

Lasers and Bose-Einstein condensates (BECs) exhibit macroscopic quantum coherence in seemingly unrelated ways. Lasers possess a well-defined global phase while the number of photons fluctuates. In BECs of atoms, instead, the number of particles is conserved and the global phase is undefined. Here, we use gate-based quantum circuits to create a unified framework that connects lasers and BEC states. Our approach relies on a scalable circuit that measures the total number of particles without destroying long-range coherence. We introduce two complementary probes of global and relative phase coherence, study how they are affected by measurements of the particle number, and implement them on a superconducting quantum computer by Rigetti. We find that particle conservation *enhances* long-range phase coherence, highlighting a mechanism used by superfluids and superconductors to gain phase stiffness.

DOI: 10.1103/PhysRevLett.130.060403

Introduction.—One of the fundamental principles of quantum mechanics is that the number and the phase operators are canonical conjugates [1]. Accordingly, in systems with fixed numbers of particles, such as physical gases and liquids, the global phase operator has maximal uncertainty. This simple observation seems to contradict our basic understanding of Bose-Einstein condensates (BECs), superfluids, and superconductors, where phase coherence emerges in spite of particle-number conservation. This apparent contradiction is resolved by noting that, in these systems, the phase coherence is imprinted in *relative* degrees of freedom, which are unaffected by this uncertainty principle. As a consequence, to probe the phase coherence of a BEC, it is always necessary to perform an interferometric experiment between two parts of the system [2].

Long-range coherence also occurs in systems that do not conserve the total number of particles. The simplest example is a laser, where the total number of photons fluctuates, and the global phase is well-defined and can be probed directly. An intermediate situation between BECs and lasers is offered by BECs of light in optical cavities, such as BECs of exciton-polaritons [9,10] and the BECs of photons in dye molecules [11–13]. In these systems, cavities increase the lifetime of the photons, making their number a quasiconserved quantity and, under suitable conditions, allowing them to reach a BEC state. Unlike BECs of atoms, in BECs of light the total number of particles fluctuates due to cavity losses and external reservoirs [14,15]. The relation between these three many-body states (lasers, BECs of atoms, and BECs of light) has been the subject of a long-standing debate [16–20], in part due to the absence of a single platform where they can be studied on equal footing. Here, we show how to use gate-based quantum computers to create these states, and study their coherence and fluctuations.

BEC states of quantum bits.—The first step toward the simulation of many-body states of bosons using a quantum computer is to represent these states in the language of qubits. We address this challenge by considering the collective state of N qubits and focusing on their fully symmetric subspace, where the system behaves as a single spin of size $S = N/2$. We next map the state $|S = N/2, S_z = -N/2\rangle$ to the vacuum of bosons and the creation or annihilation operators to the spin rising or lowering operators $S^{\pm} = S^x \pm iS^y$ [1].

To simulate the coherent state of a laser, we use the spin-coherent state obtained by rotating each qubit in the θ direction of the XY plane:

$$|\text{coherent}\rangle = \prod_{n=1}^{N} \frac{1}{\sqrt{2}}(|0\rangle_n + e^{i\theta}|1\rangle_n). \tag{1}$$

The state $|\text{coherent}\rangle$ is an eigenstate of S^+ with eigenvalue $Ne^{i\theta}$ and is analogous to the coherent state of bosons, which is an eigenstate of a with eigenvalue $\sqrt{N}e^{i\theta}$. Accordingly, the angle θ plays the role of the global phase of the system. Without loss of generality, we focus on the case $\theta = 0$, where the spins point in the X direction and $\langle S_x\rangle = N/2$. In accordance to the number-phase canonical relation, in $|\text{coherent}\rangle$ the number of particles fluctuates, as detected by the standard deviation of S_z, $\delta S_z = \sqrt{N}/2$; see Table I.

 © 2023 American Physical Society

TABLE I. Many-body states of superconducting circuits, used to simulate long-range coherence: $|\text{dephased}\rangle$ is obtained by measuring the total S_z and $|\text{projected}\rangle$ by postselecting the $S_z = 0$ measurement outcome.

Many-body state	Qubit state	Coherence	Number fluctuations
Laser	$\|\text{coherent}\rangle$	$\langle S_x\rangle = N/2$	$\delta S_z = \sqrt{N}/2$
BEC of light	$\|\text{dephased}\rangle$	$C_N^{(2)} \approx 1/4$	$\delta S_z = \sqrt{N}/2$
BEC of atoms	$\|\text{projected}\rangle$	$C_N^{(2)} \approx 1/4$	$\delta S_z = 0$

We now move to BECs of light, which can be prepared in states where both the global phase and the total number of particles strongly fluctuate [14,15]. In our systems, such state can be obtained by measuring S_z and keeping all possible outcomes of the measurement. The resulting state is described by the density matrix

$$\rho_{\text{dephased}} = \sum_{s=-N/2}^{N/2} \delta_{S_z,s} |\text{coherent}\rangle\langle\text{coherent}|\delta_{S_z,s}, \quad (2)$$

where $\delta_{S_z,s}$ is the projection operator defined by $\lim_{\epsilon\to 0}(\epsilon/\pi)/[(S_z - s)^2 + \epsilon^2]$, or any equivalent definition of a delta function. For brevity, we will denote this state by $|\text{dephased}\rangle$, in spite of being mixed. In BECs of light, the total number of particles is measured by external baths or reservoirs, while in our simulator we will achieve this goal using ancilla qubits. The state $|\text{dephased}\rangle$ can alternatively be obtained by setting the global phase θ in Eq. (1) to be a random variable with uniform distribution in $[0, 2\pi)$ and averaging over all possible outcomes. In what follows, we will show that this state is nevertheless characterized by long-range phase coherence.

Finally, to simulate BECs of atoms, we project $|\text{coherent}\rangle$ to a subspace with a well-defined number of particles. For concreteness, we assume that the N is even and consider the projection over the subspace with $N/2$ atoms, or equivalently $S_z = 0$,

$$|\text{projected}\rangle = \mathcal{A}\delta_{S_z,0}|\text{coherent}\rangle = |S, S_z = 0\rangle, \quad (3)$$

where $\mathcal{A}$ is a normalization factor. In the case of $N = 2$ qubits, one has $|\text{coherent}\rangle = \frac{1}{2}(|0\rangle + e^{i\theta}|1\rangle)(|0\rangle + e^{i\theta}|1\rangle)$. By postselecting the state with $S_z = 0$, one obtains the Bell state $|\text{projected}\rangle = e^{i\theta}(|01\rangle + |10\rangle)/\sqrt{2}$, which is invariant under the phase rotation $\theta \to \theta + \Delta\theta$ [1]. Interestingly, this procedure allows one to create entanglement between two qubits without having them interact directly, as proposed in Ref. [21] and experimentally realized with superconducting circuits in Ref. [22]. Here, we aim at extending this analysis to large numbers of particles and studying their long-range coherence [1].

Probing long-range coherence.—In analogy to the case of a laser, the coherence of $|\text{coherent}\rangle$ can be directly measured by probing the expectation values of the spin operator $\langle S_x\rangle = N/2$. In contrast, for BEC states, the global phase is undefined and $\langle S_x\rangle = 0$. We now discuss two complementary methods to probe the phase coherence of these states.

The first method targets the phase correlations between the qubits. In the two-qubit Bell state, the relative phase is probed by a finite expectation value of the operator $\langle\sigma_1^+\sigma_2^- + \sigma_2^+\sigma_1^-\rangle = 1$, where $\sigma_i^\pm$ are the rising or lowering operators of the ith qubit. The many-body generalization of this probe is the two-point correlator

$$C_N^{(2)} = \frac{1}{2N^2}\langle S^+S^- + S^-S^+\rangle. \quad (4)$$

By expressing $S^\pm = \sum_i \sigma_i^\pm$, we obtain that $C_N^{(2)}$ is the sum of two-point correlations between each pair of qubits. In this Letter, we consider states with $\langle S_z\rangle = 0$, for which $C_N^{(2)} = \langle S_x^2 + S_y^2\rangle/N^2$ [23]. From a theoretical perspective, a quantum state is phase coherent if $C_N^{(2)}$ remains finite in the limit of $N \to \infty$. In the technical language, this situation corresponds to the spontaneous breaking of the $U(1)$ gauge symmetry associated with particle-number conservation, also known as off-diagonal long-range order [24].

We now show that the three states—$|\text{coherent}\rangle$, $|\text{dephased}\rangle$, and $|\text{projected}\rangle$—have long-range coherence. Because these states belong to the fully symmetric subspace with $S^2 = N(N+2)/4$, their coherence is related to the variance of S_z through $C_N^{(2)} = \langle S_x^2\rangle + \langle S_y^2\rangle = \langle S^2\rangle - \langle S_z^2\rangle$. In $|\text{coherent}\rangle$, the qubits are uncorrelated, such that $\langle S_z^2\rangle = \sum_i\langle(\sigma_i^z)^2\rangle = N/4$ and

$$C_{N,\text{coherent}}^{(2)} = \frac{N+1}{4N}. \quad (5)$$

The dephasing process that leads to $|\text{dephased}\rangle$ preserves S_z and, hence, leaves the coherence unchanged:

$$C_{N,\text{dephased}}^{(2)} = C_{N,\text{coherent}}^{(2)}. \quad (6)$$

Finally, during the creation of $|\text{projected}\rangle$, $\langle S_z^2\rangle$ is reduced from $N/4$ to zero. Accordingly, $\langle S_x^2 + S_y^2\rangle$ is increased by $N/4$, leading to

$$C_{N,\text{projected}}^{(2)} = \frac{N+2}{4N}. \quad (7)$$

In the thermodynamic limit ($N \to \infty$), Eqs. (5)–(7) tend to the same value: $1/4$. This is a signature of the thermodynamic equivalence of the canonical and grand-canonical ensembles. Interestingly, for any finite N the projected state is *more* coherent than the dephased one, $C_{N,\text{projected}}^{(2)} > C_{N,\text{dephased}}^{(2)}$. We can explain this effect by noting that in $|\text{dephased}\rangle$ there is a finite probability to find a state with no particles

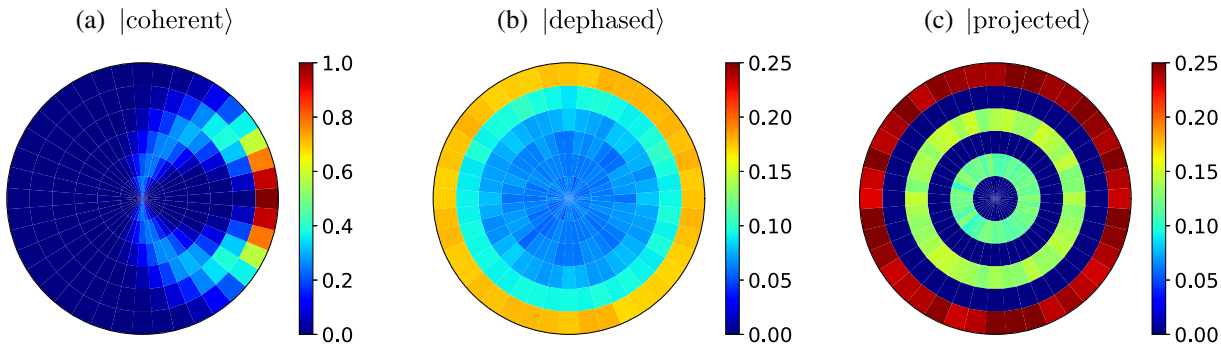

FIG. 1. Probability distribution of the operator S_θ, defined in Eq. (8), for a system of $N = 10$ qubits in the states (a) $|\text{coherent}\rangle$, (b) $|\text{dephased}\rangle$, (c) $|\text{projected}\rangle$. The angular coordinate corresponds to θ and the radial coordinate to the size of $S_\theta \in [-N/2, N/2]$. The color coding represents the probability of observing a specific value of S_θ for a fixed θ. Long-range coherence is signaled by the large absolute values of S_θ.

($|S_z = -N/2\rangle$), which does not possess any coherence. In contrast, $|\text{projected}\rangle$ includes only states with $N/2$ particles and its coherence is the maximum attainable one.

We now move to a second method to probe the coherence of the BEC states based on the probability distribution of physical observables, a method often referred to as full counting statistics [25]. As explained above, a BEC state is characterized by $\langle S_x\rangle = \langle S_y\rangle = 0$ along with large values of $\langle S_x^2 + S_y^2\rangle$. This is possible only if S_x and S_y have bimodal distributions with a high probability of finding large absolute values. To address the gauge invariance of the state, we probe the spin operator in a generic direction θ on the XY plane, defined as

$$S_\theta = \cos(\theta)S_x + \sin(\theta)S_y. \tag{8}$$

Figure 1 shows the discrete probability function of S_θ for the three states of Table I in a system with $N = 10$ particles, using a color map in polar coordinates: the angular coordinate of these graphs is θ and probes to the global phase of the condensate; the radial coordinate refers to the possible values of $S_\theta = -N/2, \ldots, N/2$. The latter is related to the coherence parameter by $C_N^{(2)} = \pi^{-1}\int_0^{2\pi} d\theta \langle S_\theta^2\rangle/N^2$. The distribution probability of S_θ can be probed by measuring the components of each qubit in the θ direction of the XY plane and summing the results [1,30].

The color map corresponding to $|\text{coherent}\rangle$, Fig. 1(a), is strongly peaked at $\theta = 0$ and demonstrates that this state has a well-defined global phase. In contrast, the color maps of the BEC states $|\text{dephased}\rangle$ and $|\text{projected}\rangle$ are rotational symmetric and do not have a well-defined global phase. Their long-range coherence is signaled by the large probability to measure $|S_\theta| = N/2$ (i.e., the outermost rings). The two states can be distinguished by their different radial dependence: In $|\text{dephased}\rangle$ the probability distribution is a monotonously increasing function of $|S_\theta|$, while in $|\text{projected}\rangle$ the probability of observing $S_\theta = s$ exactly vanishes if $s - N/2$ is an even number, giving rise to a nonmonotonous behavior. The proof of this selection rule relies on the conservation of the number of particles. Hence, the difference between odd and even rings can be used as a probe of the suppression of the fluctuations of the number of particles in $|\text{projected}\rangle$ with respect to $|\text{dephased}\rangle$.

Algorithms for an ideal quantum computer.—BEC states of atoms and photons can be prepared deterministically by, first, rotating each qubit in the $|+\rangle$ state, giving rise to $|\text{coherent}\rangle$, and then measuring S_z. To obtain the state $|\text{projected}\rangle$ it is further necessary to postselect the outcomes with $S_z = 0$. Importantly, the probability of obtaining this value is lower bounded by $1/N$, showing that the number of measurements required to obtain a fixed precision grows linearly with the number of qubits (and not linearly with the size of the Hilbert space).

The measurement of S_z can be achieved using $N_a = \text{floor}[\log_2(N)]$ ancilla qubits, corresponding to the binary representation of $|S_z|$ (see Ref. [31] for a related algorithm). Each ancilla qubit interacts sequentially with all the qubits, counting the total number of particles. Specifically, we propose to rotate the ath ancilla by an angle $\phi_a/2$ with $\phi = \pi/2^a$ if the qubit is in the $|1\rangle$ state, i.e., if a particle is present, or by $-\phi_a/2$ if the qubits is in the $|0\rangle$ state. At the end of the protocol, the ancilla is rotated by $\phi_a S_z$. The state with $S_z = 0$ is obtained by postselecting the outcomes where all the ancillas returned to their initial state [1].

In Fig. 2 we plot the value of the coherence parameters $C_N^{(2)}$ and $\langle S_x\rangle$ along the process of creating the states $|\text{dephased}\rangle$ and $|\text{projected}\rangle$, starting from $|\text{coherent}\rangle$. At each step, we couple one additional qubit to the ancillas. We observe that $\langle S_x\rangle$ decreases monotonously and tends to zero, while $C_N^{(2)}$ has a nonmonotonous behavior and tends to Eq. (7) or Eq. (6), depending on whether the value of the ancillas is postselected or not. At the end of this protocol, the probability function of S_θ corresponds to Figs. 1(c) or 1(b), accordingly. These plots can be used to check that the protocol has successfully prepared the states $|\text{projected}\rangle$ or $|\text{dephased}\rangle$, corresponding to, respectively, a BEC of atoms and a BEC of light.

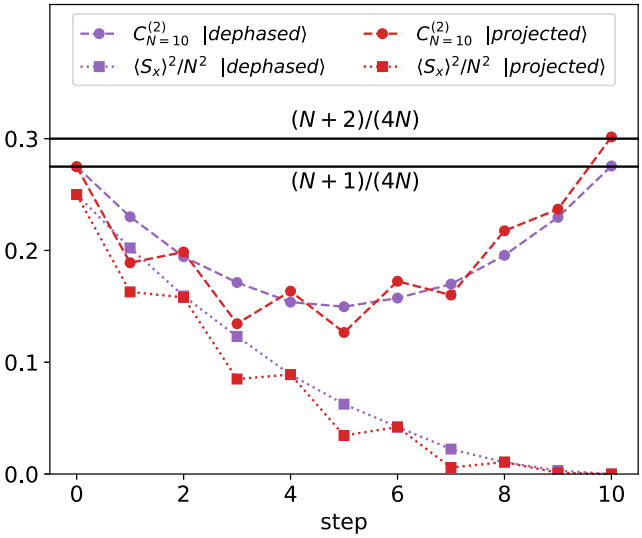

FIG. 2. Coherence parameters, $C_N^{(2)}$ and $\langle S_x\rangle$, as a function of the number of qubits coupled to the ancillas for a state with $N = 10$ qubits and $N_a = 3$ ancillas. The red (purple) curves refer to situation where all the ancilla are (not) postselected, leading to the creation of the state $|\text{projected}\rangle$ ($|\text{dephased}\rangle$). The horizontal lines correspond to the $C_N^{(2)}$ values for these states [Eqs. (6) and (7)].

Implementation on a real quantum computer.—To realize this protocol in a superconducting quantum computer, we need to overcome several difficulties. First, in these systems each qubit is coupled to at most three other qubits. Hence, a single ancilla cannot be coupled with all the other qubits at the same time. This problem can be solved in a scalable way by considering a linear chain of qubits, such that the ancillas are initially located at one side of the chain. At each step, every ancilla interacts with a neighboring qubit and is then swapped with the qubit. We will refer to the combination of the controlled rotation of the ancilla and the qubit-ancilla swap as aSWAP gate and explain below how to implement it using native gates.

A common challenge of near-term quantum computing is to compile proposed algorithms using as few native two-qubit gates as possible. First, we note that the controlled-rotation CRX(ϕ) gate is usually not a native gate. To overcome this difficulty, we first rotate the ancillas in the X direction, then use CPHASE(ϕ) gates to rotate the ancillas around the Z axis, and, finally, measure them in the X basis. The resulting circuit for the case of $N = 4$ qubits and $N_a = 1$ ancillas is shown in Fig. 3(a). In the first layer, the upper Hadamard (H) gate prepares the ancilla in the X direction and the lower four prepare the qubits in the state $|\text{coherent}\rangle$. At the end of the circuit, the first four qubits are found in a BEC state and are measured in the θ direction of the XY plane to probe S_θ. The last qubit represents the ancilla and is measured in the X direction. The aSWAP gates can be implemented using native gates for the Rigetti quantum computers, namely RZ, CPHASE, and iSWAP [see Fig. 3(b)], giving rise to a circuit with $2NN_a$ two-qubit gates.

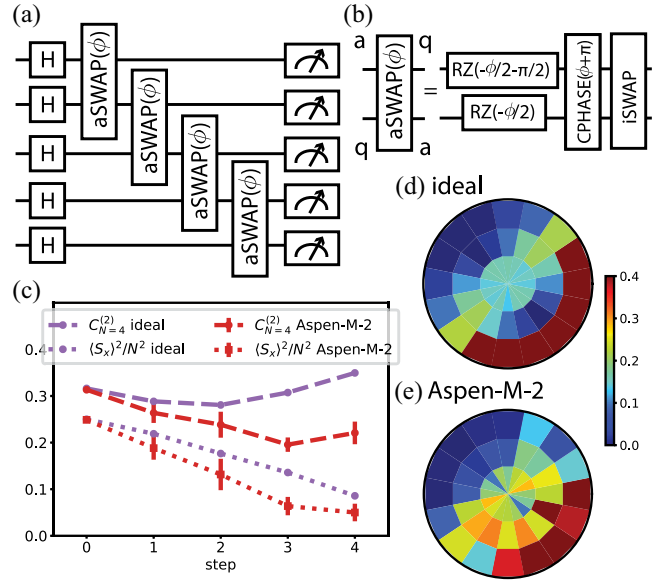

FIG. 3. (a) Circuit used to prepare a BEC state with $N = 4$ qubits and $N_a = 1$ ancilla. The aSWAP gate performs a controlled rotation of the ancilla and moves it to the next qubit. (b) Implementation of the aSWAP gate (see text) using native gates. (c) Coherence parameters as a function of the entangling gates for the state $|\text{projected}\rangle$, obtained by the protocol in (a), in the ideal circuit and in Aspen-M-2. The error bars refer to an average over three separate runs with $N = 1000$ shots each. (d)–(e) Probability distribution of S_θ in the final state of the protocol in (a).

Using the latest quantum processor by Rigetti, Aspen-M-2, we were able to implement this circuit and obtain satisfactory results for $N = 4$ and $N_a = 1$. To improve our results, we reduced the total number of gates by avoiding swapping the ancilla with the first and last qubit, obtaining a circuit with six two-qubit gates only [1]. We used a rotation angle of $\phi = \pi/2$ such that the ancilla's postselection allowed us to project out the states $S_z = \pm 2$ and suppress the fluctuations of S_z. The resulting projected state is analogous to $|\text{projected}\rangle$ and, in particular, is characterized by a reduced value of $\langle S_x\rangle = 1.17 < N/2$ and an enhanced coherence $C_4^{(2)} = 0.35 > C_{4,\text{coherent}}^{(2)}$. The probability distribution of S_θ is plotted in Fig. 3(d) and shows that the global phase spreads over approximately 90°. This is the result of using a single ancilla, instead of the two required to obtain a BEC state with an undefined global phase. The results obtained on the real hardware are in qualitative agreement with the ideal ones. In particular, $\langle S_x\rangle$ is a monotonously decreasing function, while $C_N^{(2)}$ is nonmonotonous. The distribution function shows the correct radial and angular direction, demonstrating a good calibration of the hardware [1]. These results are consistent with noisy simulations that take into account finite gate fidelities and the dephasing of the qubits. We estimate that a reduction of the error rates by a factor of 2 will enable us to double the number of ancillas

and observe a BEC state with a conserved number of particles.

Conclusion.—In this Letter, we proposed and realized quantum circuits that simulate many-body states with long-range coherence. A key aspect of our approch is an efficient algorithm that measures the total number of particles without destroying the phase coherence. Our protocol scales favorably with the number of qubits (the numbers of measurements and gates scales, respectively with N and $N \log_2 N$) and can be realized in state-of-the-art quantum computers. Our study clarifies the difference between coherent states and BEC states and shows how to identify them using physical observables. We hope that this Letter will contribute to the debate on the nature of the BEC of light and its relation to lasing and superradiance.

As a key result, we found that BECs of atoms have larger coherence than coherent states: by reducing the fluctuations in the total number of particles, one obtains a state with a more phase coherence. An analogous effect occurs in superfluids and superconductors, where local interactions are required to achieve phase stiffness [1]. To study this connection in a superconducting quantum computer, we plan to prepare a coherent state of many qubits and then couple ancilla qubits to local neighbors. By measuring the ancillas and postselecting the states with a specific outcome, we will obtain an entangled state with long-range phase coherence. These correlations will be immune to local changes of the chemical potential and, hence, potentially provide a noise-free resource for quantum algorithms.

This material is based upon work supported by the U.S. Department of Energy, Office of Science, National Quantum Information Science Research Centers, Superconducting Quantum Materials and Systems Center (SQMS) under contract no. DE-AC02-07CH11359 and by Rigetti Computing. E. G. D. T. was supported by the Israeli Science Foundation Grants no. 151/19 and 154/19. We acknowledge useful discussions with Jonathan Ruhman, Eleanor Rieffel, Davide Venturelli, Sohaib Alam, Gabriel Perdue, Thomas Iadecola, Alex Hill, Nicolas Didier, Maxime Dupont, Bram Evert, Mark Hodson, and the SQMS Algorithms group.

[1] See Supplemental Material, Sec. I, at http://link.aps.org/supplemental/10.1103/PhysRevLett.130.060403 for a simple proof of the number-phase uncertainty relation; Sec. II, for more details about the mapping between spin and qubit states; Sec. III, for an explicit study of the two-qubit case; Sec. IV, for an alternative method based on Wigner distribution, Sec. V, for a proof based on the Berry curvature of spins; Sec. VI, for the selection rules in the case of $N = 10$ qubits and $N_a = 3$ ancillas; Sec. VII, for the circuit used to measure S_θ; Sec. VIII, for the use of error mitigation; Sec. IX, for more results, including the probability distributions and coherence parameters of $|\text{coherent}\rangle$, $|\text{projected}\rangle$, and $|\text{dephased}\rangle$, as well as attempts to implement the $N = 4$, $N_a = 2$ algorithm; Sec X, for a study of the main sources of error in the hardware and for an estimation of the resources required to run larger algorithms. Sec. XI, for more details about the relation between phase stiffness and suppressed number fluctuations.

[2] See, for example, Refs. [3–6] for more details about interference experiments with BEC of ultracold atoms and Refs. [7,8] for BEC of photons.

[3] E. W. Hagley, L. Deng, M. Kozuma, M. Trippenbach, Y. B. Band, M. Edwards, P. S. Julienne, K. Helmerson, S. L. Rolston, W. D. Phillips *et al.*, Measurement of the Coherence of a Bose-Einstein Condensate, Phys. Rev. Lett. **83**, 3112 (1999).

[4] I. Bloch, T. W. Hänsch, and T. Esslinger, Measurement of the spatial coherence of a trapped Bose gas at the phase transition, Nature (London) **403**, 166 (2000).

[5] Y. Shin, M. Saba, T. A. Pasquini, W. Ketterle, D. E. Pritchard, and A. E. Leanhardt, Atom Interferometry with Bose-Einstein Condensates in a Double-Well Potential, Phys. Rev. Lett. **92**, 050405 (2004).

[6] T. Schumm, S. Hofferberth, L. M. Andersson, S. Wildermuth, S. Groth, I. Bar-Joseph, J. Schmiedmayer, and P. Krüger, Matter-wave interferometry in a double well on an atom chip, Nat. Phys. **1**, 57 (2005).

[7] J. Marelic, L. F. Zajiczek, H. J. Hesten, K. H. Leung, E. Y. Ong, F. Mintert, and R. A. Nyman, Spatiotemporal coherence of non-equilibrium multimode photon condensates, New J. Phys. **18**, 103012 (2016).

[8] T. Damm, D. Dung, F. Vewinger, M. Weitz, and J. Schmitt, First-order spatial coherence measurements in a thermalized two-dimensional photonic quantum gas, Nat. Commun. **8**, 158 (2017).

[9] J. Kasprzak, M. Richard, S. Kundermann, A. Baas, P. Jeambrun, J. M. J. Keeling, F. Marchetti, M. Szymańska, R. André, J. Staehli *et al.*, Bose–Einstein condensation of exciton polaritons, Nature (London) **443**, 409 (2006).

[10] H. Deng, H. Haug, and Y. Yamamoto, Exciton-polariton Bose-Einstein condensation, Rev. Mod. Phys. **82**, 1489 (2010).

[11] J. Klaers, F. Vewinger, and M. Weitz, Thermalization of a two-dimensional photonic gas in a 'white wall' photon box, Nat. Phys. **6**, 512 (2010).

[12] J. Klaers, J. Schmitt, T. Damm, F. Vewinger, and M. Weitz, Statistical Physics of Bose-Einstein-Condensed Light in a Dye Microcavity, Phys. Rev. Lett. **108**, 160403 (2012).

[13] B. T. Walker, L. C. Flatten, H. J. Hesten, F. Mintert, D. Hunger, A. A. Trichet, J. M. Smith, and R. A. Nyman, Driven-dissipative non-equilibrium Bose–Einstein condensation of less than ten photons, Nat. Phys. **14**, 1173 (2018).

[14] V. V. Kocharovsky, V. V. Kocharovsky, M. Holthaus, C. R. Ooi, A. Svidzinsky, W. Ketterle, and M. O. Scully, Fluctuations in ideal and interacting Bose–Einstein condensates: From the laser phase transition analogy to squeezed states and Bogoliubov quasiparticles, Adv. At. Mol. Opt. Phys. **53**, 291 (2006).

[15] J. Schmitt, T. Damm, D. Dung, F. Vewinger, J. Klaers, and M. Weitz, Observation of Grand-Canonical Number Statistics in a Photon Bose-Einstein Condensate, Phys. Rev. Lett. **112**, 030401 (2014).

[16] P. Kirton and J. Keeling, Nonequilibrium Model of Photon Condensation, Phys. Rev. Lett. **111**, 100404 (2013).

[17] I. Carusotto and C. Ciuti, Quantum fluids of light, Rev. Mod. Phys. **85**, 299 (2013).

[18] T. Byrnes, N. Y. Kim, and Y. Yamamoto, Exciton–polariton condensates, Nat. Phys. **10**, 803 (2014).

[19] C.-H. Wang, M. Gullans, J. Porto, W. D. Phillips, and J. M. Taylor, Theory of Bose condensation of light via laser cooling of atoms, Phys. Rev. A **99**, 031801(R) (2019).

[20] P. Kirton, M. M. Roses, J. Keeling, and E. G. Dalla Torre, Introduction to the Dicke model: From equilibrium to nonequilibrium, and vice versa, Adv. Quantum Technol. **2**, 1800043 (2019).

[21] F. Motzoi, K. B. Whaley, and M. Sarovar, Continuous joint measurement and entanglement of qubits in remote cavities, Phys. Rev. A **92**, 032308 (2015).

[22] C. Dickel, J. J. Wesdorp, N. K. Langford, S. Peiter, R. Sagastizabal, A. Bruno, B. Criger, F. Motzoi, and L. DiCarlo, Chip-to-chip entanglement of transmon qubits using engineered measurement fields, Phys. Rev. B **97**, 064508 (2018).

[23] The operator $C_N^{(2)}$ can be easily probed by (i) measuring σ_n^x of each qubit, (ii) computing the total spin S_x and squaring the result, (iii) averaging over many realizations (shots), and (iv) repeating the procedure for S^y. The correlator [Eq. (4)] is the same used in quantum magnetism to detect mean-field XY ferromagnetic order.

[24] C. N. Yang, Concept of off-diagonal long-range order and the quantum phases of liquid he and of superconductors, Rev. Mod. Phys. **34**, 694 (1962).

[25] See, for example, Refs. [26–29] for the use of full counting statics to study the phase coherence of BEC of ultracold atoms.

[26] V. Gritsev, E. Altman, A. Polkovnikov, and E. Demler, How to study correlation functions in fluctuating Bose liquids using interference experiments, AIP Conf. Proc. **869**, 173 (2006).

[27] T. Kitagawa, S. Pielawa, A. Imambekov, J. Schmiedmayer, V. Gritsev, and E. Demler, Ramsey Interference in One-Dimensional Systems: The Full Distribution Function of Fringe Contrast as a Probe of Many-Body Dynamics, Phys. Rev. Lett. **104**, 255302 (2010).

[28] T. Kitagawa, A. Imambekov, J. Schmiedmayer, and E. Demler, The dynamics and prethermalization of one-dimensional quantum systems probed through the full distributions of quantum noise, New J. Phys. **13**, 073018 (2011).

[29] D. A. Smith, M. Gring, T. Langen, M. Kuhnert, B. Rauer, R. Geiger, T. Kitagawa, I. Mazets, E. Demler, and J. Schmiedmayer, Prethermalization revealed by the relaxation dynamics of full distribution functions, New J. Phys. **15**, 075011 (2013).

[30] In practice, this is done by (i) applying a rotation of θ around the axis S_z, (ii) performing a $\pi/2$ rotation, (iii) measuring $\sigma_i^z = s_i$ of each qubit and (iv) computing their sum $S_\theta = \sum s_i$.

[31] L. Botelho, A. Glos, A. Kundu, J. A. Miszczak, Ö. Salehi, and Z. Zimborás, Error mitigation for variational quantum algorithms through mid-circuit measurements, Phys. Rev. A **105**, 022441 (2022).